

CFD for multiphase flow in vertical risers

Tocci, Francesco; Bos, F.; Henkes, R. A.W.M.

Publication date

2017

Document Version

Final published version

Published in

Proceedings of the 18th International Conference on Multiphase Production Technology (MPT 2017)

Citation (APA)

Tocci, F., Bos, F., & Henkes, R. A. W. M. (2017). CFD for multiphase flow in vertical risers. In *Proceedings of the 18th International Conference on Multiphase Production Technology (MPT 2017)* (pp. 309-324). Article BHR-2017-309 BHR Group Limited.

Important note

To cite this publication, please use the final published version (if applicable). Please check the document version above.

Copyright

Other than for strictly personal use, it is not permitted to download, forward or distribute the text or part of it, without the consent of the author(s) and/or copyright holder(s), unless the work is under an open content license such as Creative Commons.

Takedown policy

Please contact us and provide details if you believe this document breaches copyrights. We will remove access to the work immediately and investigate your claim.

CFD for multiphase flow in vertical risers

F Tocci

Politecnico di Milano, Italy

F Bos

Dynaflow Research Group, The Netherlands

R Henkes

Shell Projects & Technology, The Netherlands

Delft University of Technology, The Netherlands

ABSTRACT

Simulation tools are used extensively for the design and for the improved operations of oil and gas production systems. Most of these simulations are carried out with steady and transient one-dimensional tools, such as PIPESIM, OLGA and LedaFlow. For some applications, however, such as flow in bends, flow in splitters, flow in headers to facilities etc. the one-dimensional assumption limits the prediction accuracy. As an alternative, Computational Fluid Dynamics (CFD) can be used, either for two-dimensional and three-dimensional configurations. The study as presented in this paper is focused on the verification and validation of CFD results for multiphase flow of gas and liquid through vertical pipe sections. The open source CFD framework OpenFOAM has been used for this purpose, employing two different multiphase flow methods. The Volume of Fluid method can be used for the capturing of the liquid-gas interfaces, while the two fluid model approach is typically used for dispersed phases. In the present study these two models were combined in a hybrid model and validated using two representative test cases for the vertical pipe. For these two test cases CFD and experimental results are available in the literature, particularly results with Fluent, as presented at a previous BHR conference [1], and with Star-CCM+ as presented in [2].

1 INTRODUCTION

Multiphase flows remain an area where the prediction through CFD (Computational Fluid Dynamics) is yet out of reach for the majority of applications. Multiphase flows are characterized by a broad range of scales, from the dispersed droplets at the micro scale up to macro scale free surface flows.

For the CFD simulation of multiphase flow the VOF model (Volume of Fluid) is suitable for segregated flow (i.e. flow with clear gas/liquid interfaces, such as stratified flow or annular flow), whereas the two-fluid model (or Euler-Euler approach) is suitable for dispersed flow (such as bubbly flow and mist flow). In complex multiphase flows in which both segregated flow and dispersed flow regions are present one would like to couple the VOF model and the two-fluid model in a hybrid version. Examples of such complex flow are churn flow and slug flow in vertical pipes. From a physical interpretation point of view, the coupling in the hybrid model is not problematic since the VOF model uses an indicator function for tracking the interface between the phases, which has the same meaning as a volume fraction variable in the two-fluid model. A good overview of methods that have been employed is described in [3].

The present study applies the hybrid model as available in the open-source CFD framework OpenFOAM. The model was applied to one of the simplest geometric configurations, which is a vertical pipe section. Nevertheless, the multiphase flow in that configuration can be complex, considering that, depending on the precise flow conditions, different flow regimes can occur (i.e. annular dispersed flow, churn flow, hydrodynamic slug flow and bubbly flow).

Two test cases are considered. The first test case consists a vertical pipe with a diameter of 50.8 mm at atmospheric pressure with a flow of air and water, for which experiments exist, as well as CFD simulations with the Fluent package using the VOF model [1]. For these conditions, the flow regime is churn flow. The second test case is a vertical pipe with a diameter of 67 mm at atmospheric pressure with a flow of air and silicon oil, for which experiments exist, as well as CFD simulations with the Star-CCM+ package using the VOF model [2]. The flow conditions in the second test case are resulting in a slug flow regime.

The main purpose of the study as described in the present paper is to assess the capabilities of present day CFD packages in predicting multiphase flow in pipeline systems. Although CFD will most likely be used for engineering design of details of pipe systems, such as bends and splitters, it is important to validate the models for the ‘simplest’ (or most basic) parts of the pipeline system, which are the horizontal and vertical pipe sections.

2 NUMERICAL METHOD

2.1 Model description

In the OpenFOAM module called *multiphaseEulerFoam*, developed by Wardle and Weller [4] and available in OpenFOAM since version 2.1, a numerical interface sharpening algorithm is implemented within the Eulerian framework. The advantage is that the same governing equations are solved in the full domain. In order to derive the conservation equations of this hybrid model, the individual phases are distinguished. This is achieved by conditioning the local equations so that contributions to the averaged conservation equation of one phase stem only from regions which contain that particular phase.

For the conditional averaging (sometimes called phase-weighted averaging), the governing equations are multiplied by a phase indicator function before the standard averaging technique is applied. The phase indicator function $I_k(x; t)$ is defined as:

$$I_k(\mathbf{x}, t)f(x) = \begin{cases} 1, & \text{if point } (\mathbf{x}; t) \text{ is in phase } k \\ 0, & \text{otherwise.} \end{cases}$$

The phase volume fraction is calculated as the probability of point $(\mathbf{x}; t)$ being in phase k :

$$\alpha_k = \overline{I_k(\mathbf{x}, t)},$$

where the overbar represents the ensemble average.

Assuming that there is no mass transfer between the phases, the conditionally phase-averaged equations for continuity and momentum for incompressible, isothermal flow are given by:

$$\frac{\partial \alpha_k}{\partial t} + \mathbf{u}_k \cdot \nabla \alpha_k = 0,$$

$$\frac{\partial(\rho_k \alpha_k \mathbf{u}_k)}{\partial t} + (\rho_k \alpha_k \mathbf{u}_k \cdot \nabla) \mathbf{u}_k = -\alpha_k \nabla p + \nabla \cdot (\mu_k \alpha_k \nabla \mathbf{u}_k) + \rho_k \alpha_k \mathbf{g} + \mathbf{F}_{D,k} + \mathbf{F}_{S,k},$$

where ρ_k , α_k , \mathbf{u}_k are the density, phase fraction and velocity, respectively, for phase k , and \mathbf{g} is the gravity vector, respectively. The two interfacial forces are the drag force $\mathbf{F}_{D,k}$ and the surface tension force $\mathbf{F}_{S,k}$.

The solver has a flexible algorithm that is able to give a sharp interface between the phases. The interface sharpening method of Weller [5] is employed, wherein an additional term is added in the following way:

$$\frac{\partial \alpha_k}{\partial t} + \mathbf{u}_k \cdot \nabla \alpha_k + \nabla \cdot (\mathbf{u}_c \alpha_k (1 - \alpha_k)) = 0.$$

The interface compression scheme of Weller adds an additional term to the LHS of the volume fraction transport equation. This additional convective term is referred to as the compression term (named after its role to compress the free surface towards a sharper one). The value for the artificial interface compression velocity, \mathbf{u}_c , is given by:

$$\mathbf{u}_c = C_\alpha |\mathbf{u}| \frac{\nabla \alpha}{|\nabla \alpha|},$$

\mathbf{u}_c is applied in the direction normal to the interface to compress the volume fraction field and to maintain a sharp interface. The term $\alpha_k(1 - \alpha_k)$ ensures that it is only active in the interface region. The coefficient C_α controls the interfacial compression which can be switched on ($C_\alpha = 1$) or off ($C_\alpha = 0$). With C_α set to 0 for a given phase pair, there is no imposed interface compression which will result in phase dispersion according to the two-fluid (Euler-Euler) model. In contrast to this when it is set to 1, sharp interface capturing is applied and VOF-style phase fraction capturing occurs. In this work C_α is taken equal to 1.

The surface tension at the gas-liquid interface generates an additional pressure gradient (or jump), which is evaluated using the Continuum Surface Force (CSF) model. This model interprets the surface tension as a continuous, three dimensional effect across an interface, rather than as a boundary value condition on the interface:

$$\mathbf{F}_{S,k} = \sigma \kappa \nabla \alpha,$$

where σ is the fluid surface tension coefficient and κ is the local surface curvature determined from:

$$\kappa = -\nabla \cdot \left(\frac{\nabla \alpha}{|\nabla \alpha|} \right).$$

The interface drag represents the resistance opposed to the bubble motion in the fluid (or, more generally, the resistance due to the relative motion between two phases). The drag force clearly depends on the bubbles size (i.e. a larger bubble experiences a larger drag force) and the relative velocity between the two phases. The drag term $\mathbf{F}_{D,k}$ is given by:

$$\mathbf{F}_{D,k} = \alpha_c \alpha_d K (\mathbf{u}_d - \mathbf{u}_c),$$

where the subscripts c and d denote the continuous and dispersed phase values and K is given by:

$$K = \frac{3}{4} \rho_c C_D \frac{|\mathbf{u}_d - \mathbf{u}_c|}{d_d}.$$

The model of Schiller and Naumann is used:

$$C_D = f(x) = \begin{cases} \frac{24(1 + 0.15Re^{0.683})}{Re}, & Re < 1000 \\ 0.44, & Re \geq 1000. \end{cases}$$

The *multiphaseEulerFoam* module contains two diameter models: constant and isothermal. The isothermal model is used in the present paper, assuming the change of state to be isothermal. Gas bubbles change their diameter as the ambient pressure changes, based on the specified gas law.

To ensure convergence for a time-marching solver a restriction on the Courant number is incorporated to limit the maximum time step. The *multiphaseEulerFoam* module uses an adjustable time step which is based on the maximum Courant number in the domain. The definition of the Courant number for n degrees of freedom is given by:

$$C_o = \Delta t \sum_{i=1}^n \frac{u_i}{\Delta x_i}.$$

It is generally recommended to keep the maximum local Courant number much below unity.

In OpenFOAM the turbulence can be resolved by either using RANS (Reynolds-Averaged Navier-Stokes) or by using a Large Eddy Simulation (LES) with the Smagorinsky sub-grid model for the mixture. These two approaches were originally developed for turbulence modeling in single-phase flow. However, for the two-fluid (Euler-Euler) formulation it is more rigorous to have a turbulence model per phase and to use inter-phase turbulence exchange. In this study the release version of *multiphaseEulerFoam* has been modified in order to use RANS models for the mixture.

2.2 Solution procedure

The solution procedure starts with updating the time step according to the Courant number limit and then solving the coupled set of volume fraction equations with interface sharpening for the selected phase pairs. The drag coefficients are computed and an equation for the phase velocities is constructed and resolved for initial values. The Pressure Implicit with Splitting of Operators (PISO) algorithm is used to solve the pressure-velocity coupling. PISO requires that the solution must converge at every time step. It was found that one solution step and one pressure correction was sufficient to obtain convergence.

In order to ensure phase conservation for the coupled phase fractions with added interface sharpening, limiters on the phase fraction, as well as on the sum of the phase fractions, are incorporated prior to the explicit solution of the phase fraction equation system. These additional limiters have been incorporated in a new multiphase implementation of the Multidimensional Universal Limiter with Explicit Solution (MULES). The MULES algorithm handles the boundedness property by first limiting the flux transport and then solves for the phase fraction. Limiting the flux transport is

important since large transport of fluxes from a cell may drive the volume fraction in a particular cell below zero during a single time step.

3 CASE 1

3.1 Case description

Worthen and Henkes [1] carried out CFD simulations with ANSYS Fluent 15.0 for the splitting of two-phase, gas-liquid flow from a horizontal flowline into two vertical risers. The simulated flow conditions were identical as used in the air-water experiments at the Shell Technology Centre Amsterdam. In addition to the splitter geometry, the flow through a vertical pipe only with fixed inlet boundary condition was simulated (and measured), as is illustrated in Figure 1. The latter is the case study that is also considered in the present paper. The outlet of the pipe in the CFD model is located 50D (2.54 m) downstream of the inlet. The liquid holdup fraction at the inlet was set to 0.18 which is the value predicted by the Shell Flow Explorer tool (SFE version 6.0). The inlet flow rate of the gas and liquid, respectively, were specified as:

$$Q_{air} = 31.1 \text{ m}^3/\text{h} \quad \text{and} \quad Q_{water} = 1 \text{ m}^3/\text{h}.$$

The nominal pipe diameter was 50.8 mm such that the superficial velocities become:

$$U_{s,air} = 4.26 \text{ m/s} \quad \text{and} \quad U_{s,water} = 0.137 \text{ m/s}.$$

The relevant fluid properties are:

$$\begin{aligned} \rho_{air} &= 1.25 \text{ kg/m}^3 & \text{and} & \quad \mu_{air} = 0.0178 \text{ cP}, \\ \rho_{water} &= 999 \frac{\text{kg}}{\text{m}^3} & \text{and} & \quad \mu_{water} = 1.3 \text{ cP}. \end{aligned}$$

The air-water surface tension is specified as 0.0742 N/m.

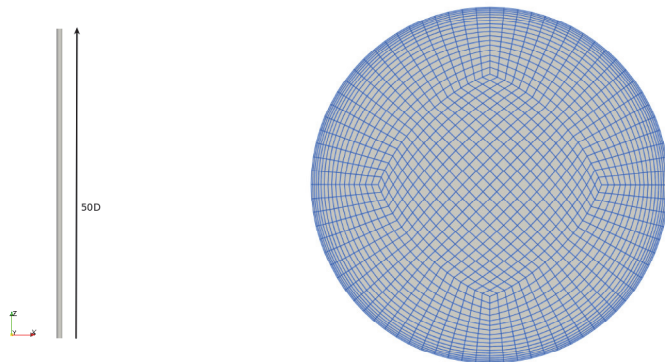


Figure 1. Case 1: setup (left) and cross-sectional grid (right) in the computational domain.

The liquid enters the domain as an annular film while the gas enters through the core. The two distinct phases are flowing upwards and discharge through the outlet to atmospheric pressure. The same conditions are imposed in the simulation with

OpenFOAM. In the Fluent simulations of [1] a total flow time of 9 s was simulated while in the present study the physical time used was 14 s. This time interval allows for the flow stabilization. The liquid holdup and pressure drop were only calculated over the last 30D of pipe length to ensure a more fully developed flow. The same quantities as considered with Fluent are calculated from the present OpenFOAM simulations in order to compare the results.

An O-grid was used, which allows for refining the mesh close to the wall and prevents a singularity at the centre of the pipe. In this grid, a Cartesian mesh is used in the centre of the pipe combined with a cylindrical one around it. The computational mesh contains 563,200 hexahedral cells. The number of cells along the axis of the pipe was chosen to be uniform.

Neither the VOF model nor the two-fluid model was found to be applicable for this problem. Ideally one wants to track the interface, at least for the large scales of the annular liquid film, but the mesh density was found to be too coarse for the dispersed phase. Therefore, a combination of the models provided by *multiphaseEulerFoam* has been used to resolve all different multiphase length scales. Turbulence was modelled using the RANS equations with the SST $k-\omega$ model for the mixture, with wall functions.

The flow rates were prescribed at the inlet through the superficial velocities and by means of the liquid hold-up. To specify the liquid holdup a value for the void fraction of 1 was defined for the annular film and 0 in the gas core. At the wall the no slip condition was applied for the velocity. At the outlet the pressure was fixed at the atmospheric value. As an initial condition the riser contained gas at zero velocity.

For the time discretization the implicit Euler scheme was used, which had a first order accuracy. For the discretization of the gradient terms the least-squares scheme was used with gradient limiters to avoid over and under shoots in the gradient computations. For the Laplacian terms the Gauss linear limited corrected scheme was adopted. The discretization of the divergence terms was specified with the Gauss scheme with the Van Leer limiter (strictly bounded between 0 and 1) and with the linear interpolation scheme. To solve the pressure equation, the geometric-algebraic multi-grid solver was chosen. The pressure and velocity fields were coupled by the PISO algorithm. The time step was adjusted according to the largest possible value, while still fulfilling the Courant number criterion; the maximum Courant number was set to 0.2, a generally accepted value for multiphase CFD flow problems. The upper limit on the time step was set to $5e-6$ s, which decreased the maximum Courant number to ~ 0.03 during the simulation. This was done to increase the stability of the simulation and to improve the convergence.

3.2 Results

In the experiments the gas flow was too low to obtain annular flow in the riser and instead the observed flow condition was churn flow; as shown in Figure 2, this churn flow was also predicted by the hybrid model.



Figure 2. CFD results for Case 1, obtained with OpenFOAM (hybrid model) for the flow pattern in the vertical pipe at $t=10$ s. Regions with a water void fraction larger than 0.5 are coloured blue.

Figure 3 shows the time dependent void fraction (averaged over the cross sectional area of the pipe) at 30D from the inlet, which exhibits the passage of the liquid structures within the flow. Note that the area-weighted average of the void fraction is computed as:

$$\frac{1}{A} \int \alpha A = \frac{1}{A} \sum_{i=1}^n \alpha_i A_i,$$

where the sum is extended to all the faces of the cells that lie on the measurement section.

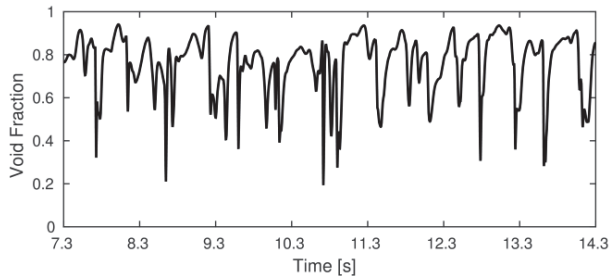


Figure 3. CFD results for Case 1. Time dependent void fraction (averaged over the cross section) obtained with the hybrid model in OpenFOAM at 30D from the inlet.

The time evolution of the total liquid holdup fraction in the pipe over 50D length is shown in Figure 4. For this case the experimental results available are the pressure drop and the liquid holdup fraction. In Table 1 the results of the present OpenFOAM simulations are compared with the results obtained with Fluent, OLGA and the experiments conducted at Shell (see [1]). The liquid holdup was not measured but it was estimated based on the measured pressure drop across the riser, assuming that the pressure drop was solely due to gravity (i.e. the frictional pressure drop was assumed negligible). There is very good agreement between the VOF results obtained with Fluent and the VOF results obtained with OpenFOAM, but there is a larger difference for both CFD results compared to the experimental values. This disagreement is attributed to the failure of the VOF method to predict slug flow in the risers; the VOF approach required very high mesh density to capture the slug interface sufficiently accurate. On the contrary, the results with the hybrid model in OpenFOAM closely agree with the experiments for both the pressure drop and the liquid hold-up.

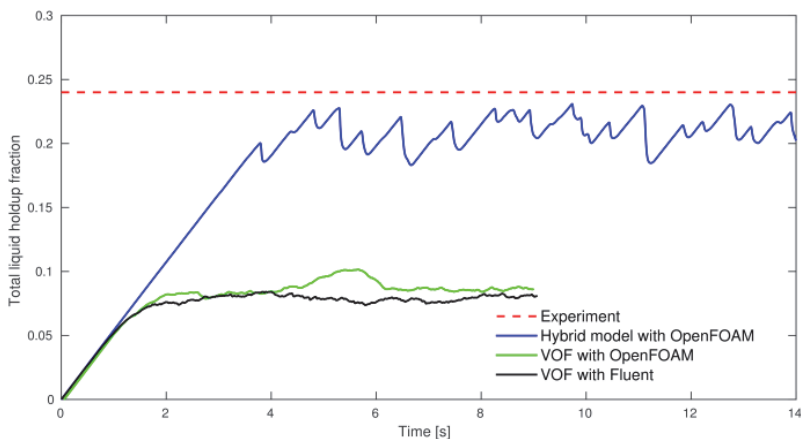


Figure 4. Total liquid holdup fraction in the 50D long vertical pipe.

Table 1. Comparison of results for Case 1: data obtained with Fluent, Shell Flow Correlations (SFC) and OLGA (see [1]) and with OpenFOAM.

	Pressure drop <i>Pa/m</i>	Liquid hold-up fraction	Flow regime
Experiments [1]	2400	0.24	Churn/Slug
OpenFOAM Hybrid	2370	0.21	Churn
OpenFOAM VOF	865	0.074	Intermittent
Fluent VOF [1]	860	0.072	Intermittent
OLGA 7.2.2 [1]	1250	0.19	Slug
Shell FC [1]	1050	0.18	Slug

The values of the pressure drop and the liquid holdup, as shown in Table 1, were time-averaged after a time at which the flow was considered to have become fully developed. In the Fluent simulations by Worthen & Henkes [1] the quantities were time-averaged over the time between 2 s and 9 s. From Figure 4 we can see that for the case with the *multiphaseEulerFoam* module in OpenFOAM the time to reach fully developed flow is longer than with Fluent and therefore the average is computed over a flow time from 5 s to 14 s. It seems that the OpenFOAM solver exhibits less numerical dissipation compare to the Fluent solution.

From the comparison in can be concluded that both Fluent and OpenFOAM CFD solvers employing the VOF method over predict the dispersion between the phases, which gives a too low liquid holdup fraction, which in turn also gives a too low hydrostatic head and thus a too low pressure drop. In contrast to this, the hybrid model as used in *multiphaseEulerFoam* in OpenFOAM is able to capture the churn flow structures from the experiments reasonably accurate.

4 CASE 2

4.1 Case description

This second test case was based on the work of Abdulkadir et al. [2, 6, 7, 8], who compared the results obtained from experiments and CFD simulations for slug flow in a vertical riser. They carried out experiments for a 6 m vertical pipe with an 0.067 m

internal diameter using air and silicone oil. The experimental test section consisted of a transparent acrylic pipe and the flow patterns were recorded using electrical capacitance tomography (ECT) and wire mesh sensors (WMS). A ring with two measurement electrodes (also known as twin-plane sensors) was placed around the circumference of the riser at a given height above the injection portals at the bottom of the riser section. The use of the twin-plane sensors enabled the determination of the rise velocity of any observed Taylor bubbles and liquid slugs. The twin-plane ECT sensors were placed at a distance of 4.4 m (ECT-Plane 1) and 4.489 m (ECT-Plane 2) from the base of the riser. The capacitance WMS (WMS-Plane 3) was placed at 4.92 m away from the mixing section, at the base of the riser. In addition to the physical experiments, the authors carried out CFD simulations with Star-CD and Star-CCM+ utilizing a VOF method. For this case the VOF method in Star-CCM+ seems to provide good results. The present paper applies the hybrid model as available in the OpenFOAM framework to capture the slug flow.

Figure 5 shows the geometry for the computational flow domain. A mesh sensitivity analysis has been carried out in [2] to identify the minimum mesh density that is required to ensure that the solution is almost independent of the mesh resolution, approximately 1.1 million cells were applied for 6 m of pipe length.

The experimental data was obtained over an interval of 60 s while the CFD simulations covered 17 s both with OpenFOAM in the present work and with Star-CCM+ in [2]. About 36 days of real time computation time was required to simulate 17 seconds of physical time using OpenFOAM on a cluster of 12 processors with the upper limit on the time step set to 5e-5 s.

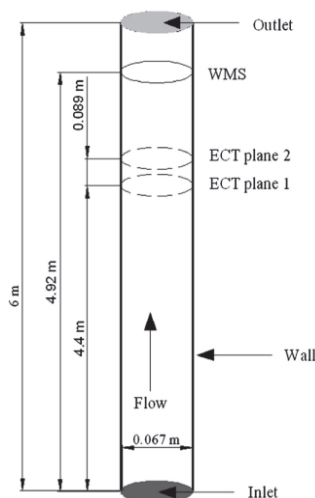


Figure 5. 3D geometry of the computational flow domain showing the locations of the sensors in the experiments.

The turbulence in the RANS approach was covered by the $k-\epsilon$ model with wall functions. At the inlet of the pipe, the mixture superficial velocity was specified. The volume fraction of each phase was specified at the inlet as a homogeneous mixture. The superficial velocities for air and oil were specified as $U_{s,air}=0.344$ m/s and $U_{s,silicone\ oil}=0.05$ m/s, respectively. At the outlet at the top of the riser, a fixed value for the pressure was specified. At $t = 0$ the riser was completely filled with liquid at zero velocity.

The relevant fluid properties are:

$$\begin{aligned} \rho_{air} &= 1.18 \text{ kg/m}^3 & \text{and} & & \mu_{air} &= 0.00018 \text{ kg/ms}, \\ \rho_{water} &= 900 \text{ kg/m}^3 & \text{and} & & \mu_{water} &= 0.0053 \text{ kg/ms}. \end{aligned}$$

The air-silicone oil surface tension is specified as 0.02 N/m.

4.2 Results

Figure 6 shows a snapshot of the simulation for the velocity field around the leading Taylor bubble rising in the stagnant silicone oil. The bubble has a round nose and fills almost the full cross sectional area of the pipe. The liquid moves around the front of the bubble as a thin liquid film moving downwards in the annular space between the pipe wall and the bubble surface. At the rear of that bubble, the liquid produces a highly agitated mixing zone in the bubble wake. This recirculation zone contains small bubbles that are shed from the bubble tail due to the turbulent jet of the liquid film.

Figure 7 shows a snapshot of the simulation for the liquid volume fraction in the fully developed slug flow. Taylor bubbles can clearly be observed followed by liquid slug bodies with dispersed small bubbles. The flow in the liquid slug body can be divided into two main parts: immediately below the rear of the bubble, where there is the formation of a recirculation and mixing region, also called wake region, and the main body of the liquid slug body where the flow is gradually recovering its original and undisturbed state. For a fully developed continuous slug flow, the length of the liquid slug bodies between any pair of consecutive bubbles remains constant and sufficiently long, which implies that the Taylor bubbles are not interacting with each other, and are rising at the same translational velocity.

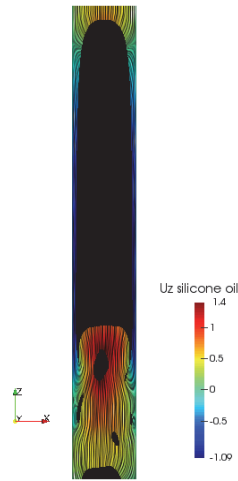


Figure 6. Simulation with OpenFOAM for the leading Taylor bubble rising through a 0.067 m internal diameter vertical pipe: instantaneous velocity field for the liquid phase.



Figure 7. Simulation with OpenFOAM for the fully developed slug flow: instantaneous void fraction.

A qualitative comparison between CFD simulations with Star-CCM+ and the experiment is demonstrated in Figure 8, as reported by Abdulkadir et al. in [2]. The comparison between the CFD simulations with OpenFOAM and the experiments is shown in Figure 9. The experimental data were kindly provided by Professor Azzopardi and Dr. Abdulkadir. From the time traces in Figure 8 and Figure 9, we can clearly distinguish the slug flow regime; there is a reasonably good agreement between the CFD and experimental results. The slug flow data shows alternating periods of high and low void fraction. High void fraction marks the gas bubble passage, and low void fraction marks the passage of the liquid slug body with some entrained dispersed gas bubbles. However, the void fraction in the liquid slug body appears to be lower in the CFD simulations compared to the experiments.

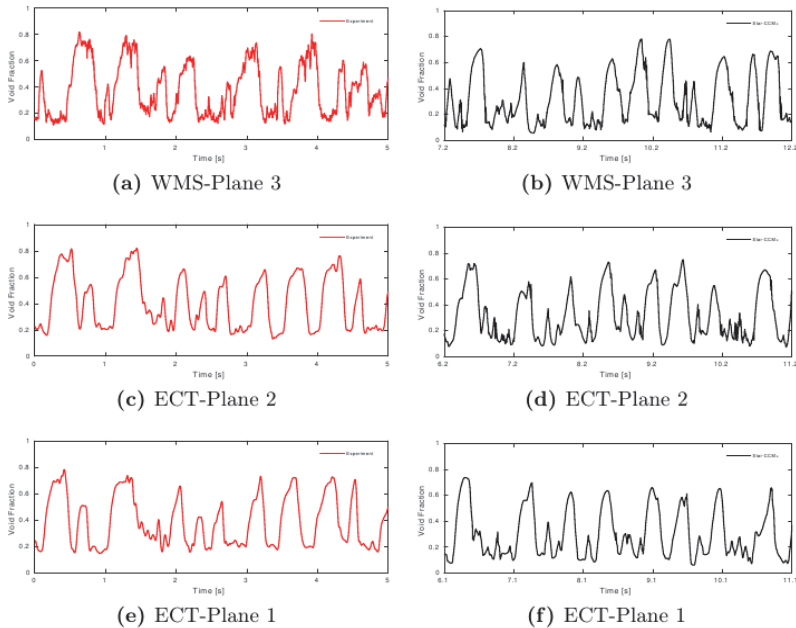


Figure 8. Comparison between experimental data (red) and CFD simulation with Star-CCM+ (black), taken from Abdulkadir et al. [2].

The time series for the void fraction as obtained from the experiments and using the OpenFOAM package are compared in Figure 9, showing a close agreement. The PDFs (Probability Density Functions) corresponding to the time series of the void fraction time series are shown in Figure 10, which includes both the simulations (with OpenFOAM and with Star-CCM+) and the experiments. There is a good agreement between the CFD simulations and the experiments in predicting the same flow pattern, being slug flow: there is a twin-peaked PDF, with one peak being characteristic for the liquid slug body and the other peak being characteristic for the Taylor bubble.

By cross-correlating the void fraction signals from ECT-Plane 1 and ECT-Plane 2 the transit time between the two section can be deduced from the measurements. Together with the distance between the measurement sections, it becomes possible to calculate the velocity of the slug unit for the fully developed flow. The time delay between the planes in the CFD predictions with OpenFOAM and the experiments is 0.08 s , while the CFD

simulations with Star-CCM+ gives 0.075 s . Dividing the distance of 0.089 m between the Plane 1 and the Plane 2 by the delay time of 0.075 s gives a slug velocity of 1.19 m/s . The slug velocity on the simulations with Star-CCM+ is slightly lower, namely 1.11 m/s .

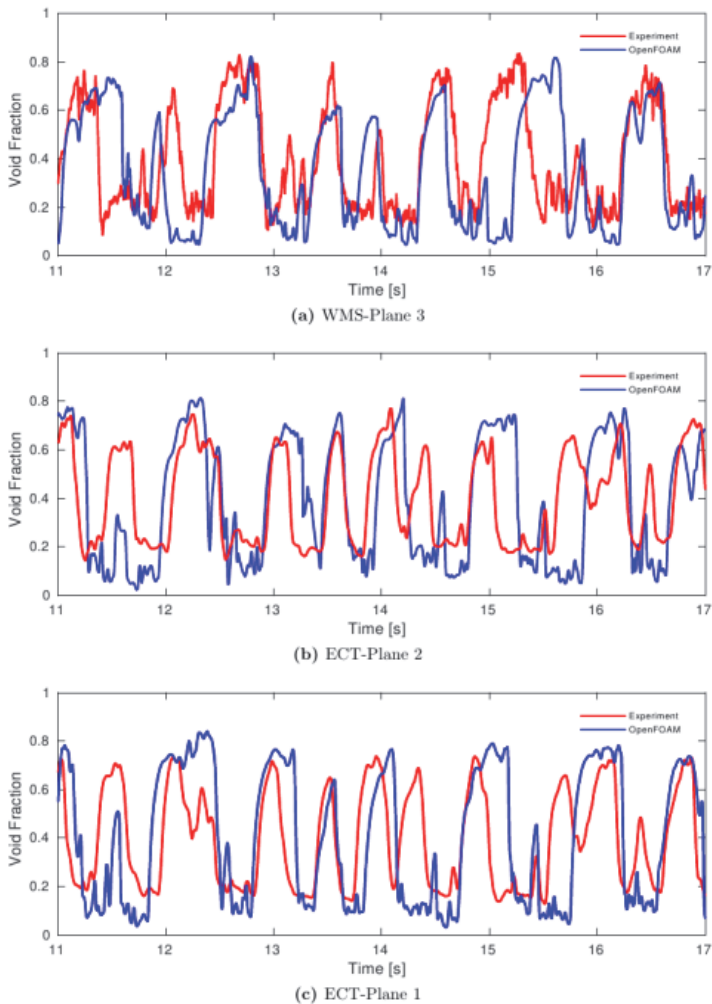


Figure 9. Time series for the void fraction in different planes; comparison between experiments and CFD simulations with OpenFOAM.

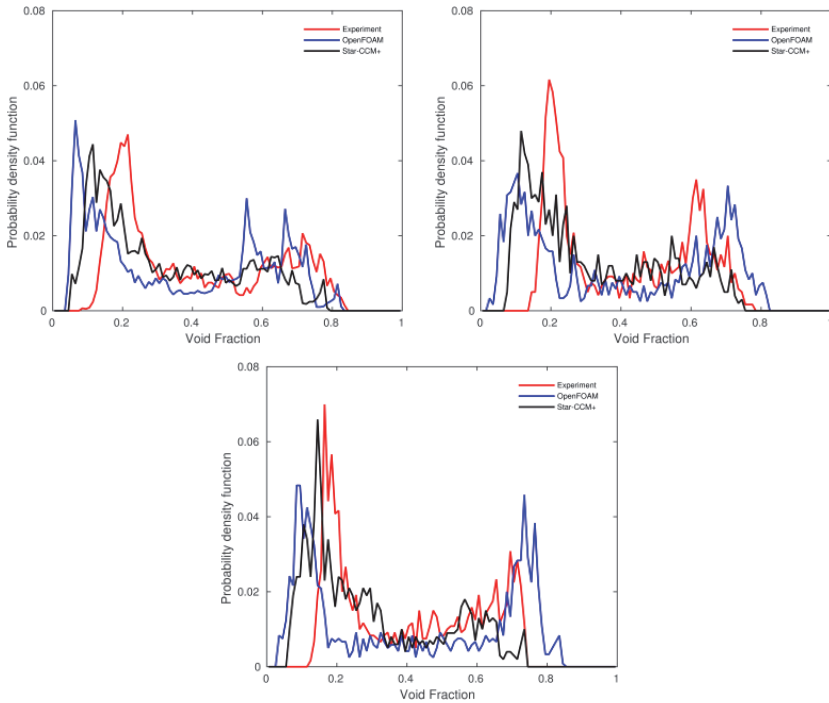


Figure 10. PDF of cross-sectional average void fraction for the case of slug flow obtained from the experiments, and from the CFD simulations with Star-CCM+ (in Abdulkadir et al. [2]) and with OpenFOAM.

Figure 11 shows a comparison for the time evolution of the void fraction between the CFD simulations and the experiments when the large leading Taylor bubble reaches the ECT-Plane 1 and the ECT-Plane 2. From that figure the void fraction in the leading Taylor bubble can be obtained. The void fraction and the liquid film thickness obtained are summarized in Table 2. The comparison between CFD simulations and experiments is again reasonably good.

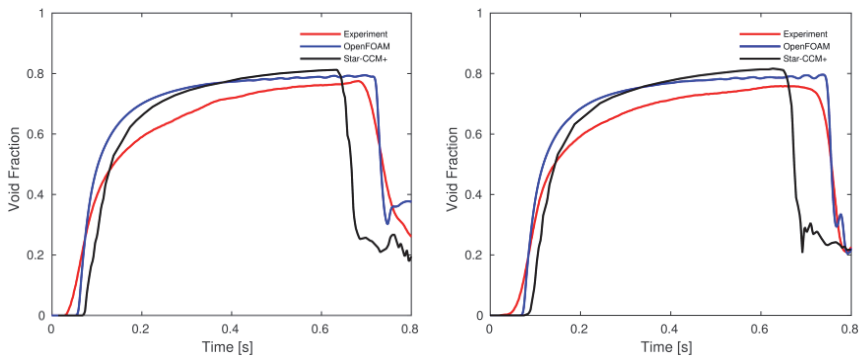


Figure 11. Comparison of the void fraction between experiments and CFD simulations with Star-CCM+ (Ref. [2]) and with OpenFOAM for the leading Taylor bubble at start-up.

Table 2. Comparison between experiments and CFD simulations with Star-CCM+ (from [2]) and with OpenFOAM for the leading Taylor bubble: void fraction and liquid film thickness.

		Experiments	OpenFOAM	Star-CCM+
Void fraction in the Taylor bubble	ECT-Plane 1	0.77	0.79	0.81
	ECT-Plane 2	0.76	0.80	0.82
Liquid film thickness [mm]	ECT-Plane 1	4.10	3.72	3.35
	ECT-Plane 2	4.30	3.54	3.16

5 CONCLUSIONS

Two-phase gas-liquid upward flow in vertical pipes or risers offers a challenge to CFD simulation methods. This is particularly the case because different flow regimes may occur, such as bubbly flow, slug flow, churn flow, or annular flow. Comparison of the simulations with experiments reveal that the Volume of Fluid (VOF) method in its original form, as available in both OpenFOAM and Fluent, is not suitable for the flow conditions that lead to slug flow or churn flow i.e. where a large slippage between the two phases exists. This shortcoming in the VOF method in OpenFOAM and Fluent shows up as an overprediction of the dispersion between the phases, or an underprediction of the liquid holdup fraction. The latter also leads to an underprediction of the hydrostatic head and consequently to a too low pressure drop.

The approach of coupling VOF with a two-fluid model is adopted and the resulting hybrid multiphase solver is now available in OpenFOAM. Within this hybrid method the VOF part keeps a sharp interface between segregated flow structures (such as a liquid film in annular flow that is separated from the gas core) and the Euler-Euler part (or the two fluid model) is able to properly represent dispersed regions, such as in bubbly flow or in the liquid slug body that has entrained gas bubbles. This makes the hybrid solver a promising approach for predicting gas-liquid flows in pipes, without a priori knowledge of the flow pattern.

The hybrid model has been applied in two examples for vertical pipe flow for which experimental data exist.

Case 1

The first case covers vertical upward churn flow of air-water through a pipe with 50.8 mm diameter. From a comparison of the results obtained from the CFD simulations in OpenFOAM and the experiments, the following conclusions can be drawn:

- The prediction by OpenFOAM using the multiphaseEulerFoam module captures the overall physics of the flow quite well. Time series of the cross-sectional averaged void fraction and contour plots of liquid holdup showed that the hybrid model was able to distinguish the flow pattern in the pipe, being churn flow.
- Very good agreement was obtained between the predictions and experiments for the pressure drop and liquid holdup fraction. The pressure drop was 2400 Pa/m in the experiments versus 2370 Pa/m in the CFD simulations. The liquid holdup fraction in the experiments was 0.24 (based on the measured pressure drop) whereas the time averaged liquid holdup fraction in the simulations was 0.21. The slightly higher value for the liquid holdup fraction in the experiments can be partly due to the assumption of zero frictional pressure drop.

Case 2

A detailed simulation of the slug flow in a 6 m vertical pipe with a 0.067 m internal diameter with air and silicone oil has been successfully carried out. The results were compared with the experimental data and with the CFD simulations with Star-CCM+ as reported in literature. The main findings are:

- The hybrid model in OpenFOAM is able to qualitatively capture the characteristics of the slug flow. Three regions were observed: the Taylor bubble, the falling film, and the wake region. The Taylor bubble is moving vertically upwards whereas the liquid film is moving downwards. In the wake region there are some entrained bubbles that are carried upwards.
- The slug flow pattern can be considered as fully developed at 4 m (60 pipe diameters).
- A reasonably good agreement between the hybrid CFD model and the experiments was obtained for the time series of cross-sectional averaged void fraction over three monitoring planes. The slug flow data had alternating periods of high and low void fraction. High void fraction marked the gas bubble passage, and low void fraction marked the passage of the liquid slug body with some entrained dispersed gas bubbles. However, the void fraction in the liquid slug body has a lower value in the CFD simulations than in the experiments.
- The agreement of the PDFs of the cross-sectional average void fraction between the CFD simulations and the experiments is quite reasonable. There is a twin-peaked PDF, with one peak being characteristic for the liquid slug body and the other peak being characteristic for the Taylor bubble. The void fraction in the liquid slug body shows a lower value in the CFD simulations than in the experiments.
- A very good agreement was found for the velocity of the slug unit for the fully developed flow between the CFD simulations with OpenFOAM and the experiments. The CFD simulations with Star-CCM+ gives a slightly lower value.
- A satisfactory agreement between the simulations and the experiments was observed for the formation and the shape of the leading Taylor bubble and for the liquid film thickness. The peak of the void fraction in the leading Taylor bubble was larger in the Star-CCM+ and OpenFOAM results than in the experiments. The length of the leading bubble was correctly predicted with OpenFOAM whereas it was a bit too low in the Star-CCM+ results.

REFERENCES

1. Worthen, R.A. and Henkes, R. A. W. M., CFD for the multiphase flow splitting from a single flowline into a dual riser, Proc. 17th Int. Conf. on Multiphase Production Technology, BHR Group, France, pp. 109–123, 2015.
2. Abdulkadir, M., Hernandez-Perez, V., Lo, S., Lowndes, I.S., Azzopardi, B.J., Comparison of experimental and Computational Fluid Dynamics (CFD) studies of slug flow in a vertical riser, Experimental Thermal and Fluid Science 68, pp. 468–483, 2015.
3. Štrubelj, L. and I. Tiselj, I., Two-fluid model with interface sharpening, Int. J. Numerical Methods in Engineering 85.5, pp. 575–590, 2011.
4. Wardle, K.E. and H.G. Weller, H.G., Hybrid multiphase CFD solver for coupled dispersed/segregated flows in liquid-liquid extraction, Int. J. Chem. Eng., 13 pages, Article ID 128936, 2013.
5. Weller, H.G., A new approach to VOF-based interface capturing methods for incompressible and compressible flow, Technical Report TR/HGW/04, 2008.

6. Abdulkadir, M., Experimental and Computational Fluid Dynamics (CFD) studies of gas-liquid flow in bends, PhD Thesis, University of Nottingham, 2011.
7. Abdulkadir, M., Hernandez-Perez, V., Lowndes, I.S., Azzopardi, B.J., Brantson, E.T., Detailed analysis of phase distributions in a vertical riser using wire mesh sensor (WMS), *Experimental Thermal and Fluid Science* 59, pp. 32–42, 2014.
8. Abdulkadir, M., Hernandez-Perez, V., Lowndes, I.S., Azzopardi, B.J., Dzomeku, S., Experimental study of the hydrodynamic behaviour of slug flow in a vertical riser, *Chemical Engineering Science* 106, pp. 60–75, 2014.